Neutrino Heating in an Inhomogneous Big Bang Nucleosynthesis Model

Juan F. Lara*

*Center for Relativity, University of Texas at Austin
Austin, Texas 78712

Abstract.
The effect of the heating of neutrinos by scattering with electrons and positrons and by $e^{-}e^{+}$ annihilation on nucleosynthesis is calculated for a spherically symmetric baryon inhomogeneous model of the universe. The model has a high baryon density core and a low density outer region. The heating effect is calculated by solving the Boltzmann Transport Equation for the distribution functions of electron and muon/tau neutrinos. For a range of baryon-to-photon ratio $\ln(\eta_{10}) = [0, 1.5]$ and $r_i = [10^2, 10^8]$ cm the heating effect increases the mass fraction $X_{^4\mathrm{He}}$ by a range of $\Delta X_{^4\mathrm{He}} = [1, 2] \times 10^{-4}$. The change of the value of $X_{^4\mathrm{He}}$ appears similiar to the change caused by an upward shift in the value of η_{10}. But the change to deuterium is a decrease in abundance ratio $Y(\mathrm{d})/Y(\mathrm{p})$ on the order of 10^{-3}, one order less than the decrease due to a shift in η_{10}.

I INTRODUCTION

When discrepencies arise between observations of light isotope abundances and the predictions of standard (homogeneous and isotropic) Big Bang Nucleosynthesis (BBN) models research has turned to BBN models with inhomogeneous baryon distributions (IBBN models) to attempt to resolve the discrepencies. Articles in the 1970's and 1980's looked for IBBN models with an overall baryon density that both equalled the critical density and satifised observational constraints on the light elements. [1] These IBBN models could not satisfy observational constraints to isotope abundances for baryon densities other than densities demanded by standard models. In the late 1990's observations of ^{4}He and deuterium placed conflicting constraints on the baryon density in standard models. (KKS, 1999) [2] found a range of agreement for the outer fringes of the 2σ ranges of the observations using an IBBN model code. Most recently (KS, 2000) [3] used an IBBN model to bring baryon density constraints from cosmic microwave background observations in agreement with constraints from ^{4}He and deuterium observations, though not with ^{7}Li observations.

Nucleosynthesis models have become more descriptive as they include smaller effects that faster computers can calculate accurately. One effect is the neutrino heating effect. Electrons and positrons pass a fraction of their energy to neutrinos through annihilation and scattering. That energy transfer can change the rates of neutron-proton interconversion, and then the results of nucleosynthesis. Hannestad and Madsen [4] derive a means of solving the Boltzmann Transport Equation for the neutrino distribution functions, presenting results for a standard BBN model. This author will discuss the neutrino heating effect in an IBBN model. This article will show how the heating effect slightly alters neutron distribution and nucleosynthesis, and show the effect's dependence on IBBN parameters.

II THE MODEL

The IBBN code for this article corresponds to a model with a spherically symmetric baryon distribution. The model is divided into a core and 31 inner shells with high baryon density, and 32 outer shells with low baryon density. A run starts at electromagnetic plasma temperature T = 100 GK. The distance scale r_i, the radius of the model when T = 100 GK, can be varied. During a run the number density $n(i,s)$ of isotope species i in shell s is determined by the equation [5]

$$\frac{dn(i,s)}{dt} = \frac{1}{n_b(s)} \sum_{j,k,l} N_i \left(-\frac{n^{N_i}(i,s) n^{N_j}(j,s)}{N_i! N_j!}[ij] + \frac{n^{N_k}(k,s) n^{N_l}(l,s)}{N_k! N_l!}[kl] \right) - 3\dot{\alpha} n(i,s) + \frac{1}{r^2}\frac{\partial}{\partial r}\left(r^2 D_n \frac{\partial n(i,s)}{\partial r} \right) \tag{1}$$

The first term corresponds to nuclear reactions and beta decays within shell s, the second term to the expansion of the universe, and the third term to diffusion of isotope i between shells. In this model only neutrons diffuse. As T falls neutrons diffuse from the high density shells to the low density shells, until the neutrons are homogeneously distributed. The weak reactions $\mathrm{n} + \nu_{\mathrm{e}} \leftrightarrow \mathrm{p} + \mathrm{e}^-$, $\mathrm{n} + \mathrm{e}^+ \leftrightarrow \mathrm{p} + \bar{\nu}_{\mathrm{e}}$, and $\mathrm{n} \leftrightarrow \mathrm{p} + \mathrm{e}^- + \bar{\nu}_{\mathrm{e}}$ convert protons in the high density shells to neutrons, which then diffuse into the low density shells where the weak reactions convert them back to protons. Nucleosynthesis occurs earlier in the high density shells, depleting neutrons. Neutrons from the low density shells then back diffuse into the high density shells until nucleosynthesis incorporates all neutrons into nuclei, mostly ^{4}He nuclei.

Figure (1a) shows the mass fraction $X_{^4\mathrm{He}}$ of ^{4}He nuclei produced by the model, as a function of η and r_i (in centimeters). Contour lines correspond to specific values of $X_{^4\mathrm{He}}$. Neutron diffusion occurs later as r_i increases. The shape of the contour lines is determined by when neutron diffusion occurs compared with the weak reaction rates mentioned above and with nucleosynthesis. As r_i increases the time of neutron diffusion coincides less and less with the time before the weak reactions fall out of equilibrium. More protons then remain in the high density

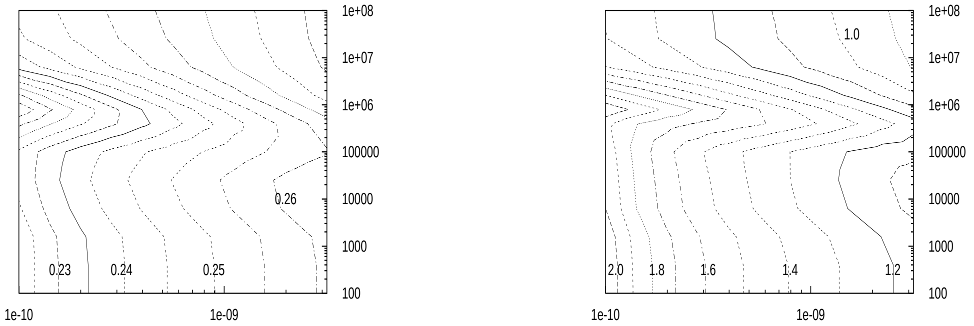

FIGURE 1. $X_{^4\mathrm{He}}$ (1a) and $10^4\Delta X_{^4\mathrm{He}}$ (1b) due to neutrino heating.

shells. When $r_i = 25000$ cm the innermost shells retain all their protons, and nucleosynthesis occurs earlier enough that nearly all neutrons back diffuse into the high density shells to undergo nucleosynthesis. $X_{^4\mathrm{He}}$ increases as r_i increases to 25000 cm. But for larger r_i neutrons cannot reach the innermost shells before nucleosynthesis, leading to decreasing production of ^{4}He. ^{4}He production bottoms out at $r_i = 790000$ cm when diffusion occurs at the same time as nucleosynthesis. For higher $r_i =$ the high density shells and the low density shells act separately from each other, with the high density shells producing large amounts of ^{4}He.

To calculate the neutrino heating effect, the model solves the Boltzmann Transport Equation [4]

$$\begin{aligned}\frac{df_1(p_1)}{dt} = {} & \frac{1}{2E_1}\left(\frac{kT_N}{R}\right)^5 \int \frac{d^3p_2}{(2\pi)^3 2E_2} \int \frac{d^3p_3}{(2\pi)^3 2E_3} \\ & \int \frac{d^3p_4}{(2\pi)^3 2E_4} S|M|^2 (2\pi)^4 \delta^4(p_1 + p_2 - p_3 - p_4) \\ & \{[1 - f_1(p_1)][1 - f_2(p_2)] f_3(p_3) f_4(p_4) \\ & - f_1(p_1) f_2(p_2)[1 - f_3(p_3)][1 - f_4(p_4)]\} \end{aligned} \qquad (2)$$

for the neutrino distribution functions $f_i(p_i)$. The distribution functions are used to calculate the neutrino energy densities, and $f_{\nu_\mathrm{e}}(p_\mathrm{e})$ for electron neutrinos is used to calculate the neutron-proton conversion reaction rates. Increased $f_{\nu_\mathrm{e}}(p_\mathrm{e})$ makes the conversion reactions produce fewer neutrons for nucleosynthesis, but decreased electron energy density ρ_e makes those reactions produce more neutrons at the same time. Decreased ρ_e decreases temperature T, making nucleosynthesis occur earlier, when more neutrons are present. This last effect, the clock effect, ultimately determines the increase in $X_{^4\mathrm{He}}$ due to neutrino heating.

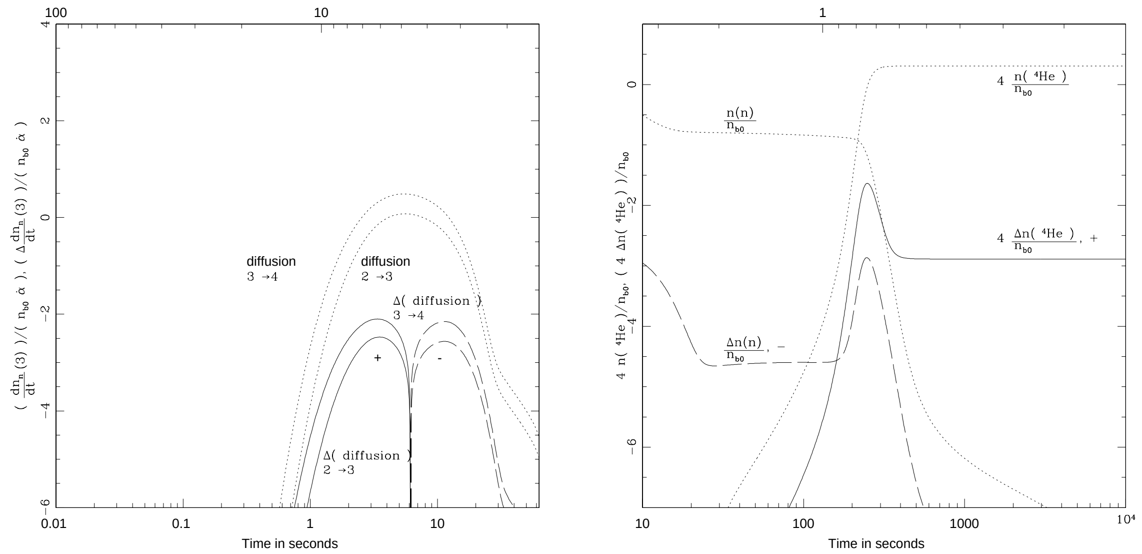

FIGURE 2. In Figure (2a) the dotted lines are the diffusion rates to and from shell 3, and the solid (increase) and dashed (decrease) lines are the changes of the rates due to neutrino heating. Figure (2b) shows $n(\mathrm{n})$ and $n(^4\mathrm{He})$ (dotted lines) and the changes in these number densities due to heating. n_{bO} is a normalizing factor and $\dot{\alpha}$ is the expansion rate of the universe.

III RESULTS

The diffusion coefficient D_n is calculated from collisions between neutrons and electrons/positrons (D_ne) and neutrons and protons (D_np). [6]

$$\frac{1}{D_\mathrm{n}} = \frac{1}{D_\mathrm{ne}} + \frac{1}{D_\mathrm{np}} \tag{3}$$

$$D_\mathrm{ne} = \frac{3}{8}\sqrt{\frac{\pi}{2}}\frac{c}{n_\mathrm{e}\sigma_\mathrm{ne}}\frac{K_2(z)}{\sqrt{z}K_{5/2}(z)}\left(1 - \frac{n_\mathrm{n}}{n_t}\right) \tag{4}$$

$$z = \frac{m_\mathrm{e}}{kT}$$

Neutrino heating affects D_ne by lowering the electron number density n_e and lowering the electromagnetic plasma temperature T at a given time. The neutrinos and the electrons/positrons are homogeneously distributed throughout this model. So D_ne is the same for all the shells.

Figure (2a) shows the neutron diffusion rates into and out of Shell 3, a high density inner shell, for the case of $\eta_{10} = 3.0$ and $r_i = 25000$ cm. Figure (2a) also shows the change in the rates due to heating. This change is at first positive, and then becomes negative. This change corresponds to a shift in the diffusion rate to a time earlier by 0.1 %. All other shells also have this earlier time shift. Figure (2b) shows the number densities of neutrons (n_n) and ^{4}He nuclei ($n_{^4\mathrm{He}}$) at around $T = 0.8$ GK, when nucleosynthesis occurs, for shell 3 and the same values of η_{10}

and r_i. Figure (2b) also shows the changes in n_{n} and $n_{^4\mathrm{He}}$ due to neutrino heating. The clock effect mentioned above is seen in the humps in the graphs for the changes Δn_{n} and $\Delta n_{^4\mathrm{He}}$. Δn_{n} and $\Delta n_{^4\mathrm{He}}$ are larger between the time when neutrons are converted to ^{4}He nuclei with the heating effect on and when neutrons are converted to ^{4}He nuclei without heating.

Figure (1b) shows $10^4 \Delta X_{^4\mathrm{He}}$, the change due to neutrino heating. For the ranges of η and r_i observed $\Delta X_{^4\mathrm{He}}$ remains within a range of $[1.1, 2.0] \times 10^{-4}$. $X_{^4\mathrm{He}}$ is determined by the baryon number densities in the shells, and those densities also determine the magnitude of the clock effect. That seems to account for the contour lines of $\Delta X_{^4\mathrm{He}}$ tracking the contour lines of $X_{^4\mathrm{He}}$ itself. The heating effect on $X_{^4\mathrm{He}}$ seems to be similar to the effect one would get by shifting the value of η upwards by about 1 to 2 %. The earlier shift in neutron diffusion due to heating would have the effect of the lines in Figure (2a) being stretched to higher values of r_i. So for a given value of r_i and η the change $\Delta X_{^4\mathrm{He}}$ will have a value corresponding to $X_{^4\mathrm{He}}$ at that point in the graph plus a shift corresponding to a lower value of r_i. The change is bigger for $r_i \leq 25000$ cm, when $X_{^4\mathrm{He}}$ decreases with decreasing r_i, and is smaller for 25000 cm $< r_i \leq$ 790000 cm when $X_{^4\mathrm{He}}$ increases with decreasing r_i.

Figure (3a) shows the overall abundance ratio $Y(\mathrm{d})/Y(\mathrm{p})$ between deuterium and protons. Figure (3b) shows $10^3 \Delta \log[Y(\mathrm{d})/Y(\mathrm{p})]$, the change due to neutrino heating. The nuclear reaction rates that create and destroy deuterium depend on the electromagnetic plasma temperature T and on shell s's baryon energy density $\rho_b(s)$. Through T neutrino heating shifts the nuclear reaction rates to a slightly earlier time. So for $r_i < 10^5$ cm less deuterium remains at the end of a run. This decrease in $Y(\mathrm{d})/Y(\mathrm{p})$ due to heating turns out to be one order of magnitude less than the decrease that would come from an increase in η_{10} mentioned above. For $\eta_{10} = 3.0$ and $r_i = 25000$ cm one has to increase η by 1.53 % to increase $X_{^4\mathrm{He}}$ by as much as neutrino heating does. But that upward shift would decrease $\log[Y(\mathrm{d})/Y(\mathrm{p})]$ by around 9.19×10^{-3}, instead of the decrease of 1.12×10^{-3} done by heating. For $r_i > 10^5$ cm the low density outer shells produce considerable amounts of deuterium. In that range the heating effect increases deuterium production. The neutrino heating effect on ^{4}He can then be distinguished from a shift in η_{10} by looking at how $Y(\mathrm{d})/Y(\mathrm{p})$ differs from the results without heating.

IV CONCLUSIONS AND FUTURE RESEARCH

The neutrino heating effect increases the mass fraction of ^{4}He by $[1.1, 2.0] \times 10^{-4}$ for the observed range of baryon-to-photon ratio $\eta_{10} = [1, 32]$ and distance scale $r_i = [10^2, 10^8]$ cm. That's the same order of magnitude as in the standard case. The increase in the mass fraction resembles the increase that would come from increasing η_{10} by about 1 % to 2 %. The heating effect also decreases deuterium production. But the decrease in deuterium is an order of magnitude less than the decrease that would come from the increase of η_{10} mentioned above. Further, the effect increases deuterium production for $r_i \geq 10^5$ cm.

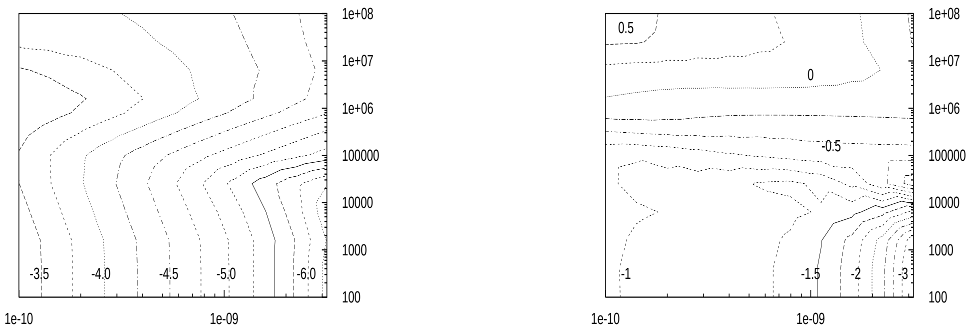

FIGURE 3. $\log[Y(\mathrm{d})/Y(\mathrm{p})]$ (3a) and $10^3\Delta\log[Y(\mathrm{d})/Y(\mathrm{p})]$ (3b) due to neutrino heating.

A larger future article can show the earlier time shift of neutron diffusion for values of η_{10} and r_i other than 3.0 and 25000 cm, and for shells other than shell 3 as well. These graphs would show how this time shift is characteristic of the whole observed range of η_{10} and r_i. The article can also look at deuterium production for r_i lower than and higher than 10^5 cm, to explain in more detail how the change due to neutrino heating changes signs. The article can also comment on production of other isotopes, such as ^{7}Li. One can determine if the change due to heating has a distance scale dependence similar to the dependence for deuterium.

One should note that CMB observations have placed parameters on the baryon-to-photon ratio ($\Omega_B h^2 = 0.032^{+0.009}_{-0.008}$ where $\Omega_B h^2 = (3.650 \pm 0.008) \times 10^{-3}\eta_{10}$) [7]. A future article should particularly look at the IBBN code's behavior in regions corresponding to these parameters.

REFERENCES

1. Malaney, R.A., and Mathews, G.J., *Phys. Repts* **229**, 147 (1993) has an exhaustive list of such articles.
2. Kainulainen, K., Kurki-Suonio, H., and Sihvola, E., *Phys. Rev.* **D59**, 083505 (1999).
3. Kurki-Suonio, H., and Sihvola, E., astro-ph/0011544.
4. Hannestad, S., and Madsen, J., *Phys. Rev.* **D52**, 1764 (1995).
5. Mathews, G.J., Meyer, B.S., Alcock, C.R., and Fuller, G.M., *ApJ* **358**, 36 (1990).
6. Kurki-Suonio, H., Aufderheide, M.B., Graziani, F., Mathews, G.J., Banerjee, B., Chitre, S.M., and Schramm, D.N., *Phys. Let.* **B289**, 211 (1992).
7. Burles, S., Nollet, K.M., and Turner, M.S., astro-ph/0008495.